Eur. Phys. J. B **13**, 561–569 (2000)

THE EUROPEAN PHYSICAL JOURNAL B

EDP Sciences

Dielectric resonances in three-dimensional binary disordered media

G. Albinet and L. Raymond[a]

I.R.P.H.E., CNRS – Universités d'Aix-Marseille I & II, Service 242, Campus Universitaire de St. Jérôme, 13397 Marseille Cedex 20, France

Received 24 March 1999

Abstract. Powdered solids often present very specific properties due to their granular nature. Such powders are often obtained by mixing two ingredients in variable proportions: conductor and insulator, or conductor and super-conductor. In a very natural way, these systems are modeled by regular lattices, whose sites or bonds are randomly chosen with given probabilities. It is known that the electrical and optical properties of random bi-dimensional (2D) networks are well described by their conductance's poles (resonances) and residues (amplitudes). The numerical implementation of a spectral method gave the spectral density, the AC conductivity, the multi-fractal properties of the moments for the local electric field (or currents), and spectrum of resonances characteristic of some small clusters (animals). This work extends the spectral method to the three-dimensional (3D) case where the problem is more complicated because the duality property and the corresponding symmetries are broken. As in the 2D-case, the two significant parameters are the ratio $h = \sigma_1/\sigma_0$ of the complex conductances σ_0 and σ_1 of both phases, and the probability p (resp. $1 - p$) of σ_0 (resp. σ_1). All the resonances lie on the negative real h-axis, *i.e.* for pure non resistive networks in the AC case. For a static (DC) system, only the value $h = 0$ (corresponding to a binary system with σ_0 finite and $\sigma_1 = 0$, or $\sigma_0 = \infty$ and σ_1 finite) can give a resonance. Some applications are proposed, in particular the ability for small clusters (animals with one, two or three bonds) to present a singular response for well identified frequencies of the incident electromagnetic field.

PACS. 66.10.Ed Ionic conduction – 66.30.Dn Theory of diffusion and ionic conduction in solids – 61.43.Gt Powders, porous materials

1 Introduction

The three-dimensional materials constituted by binary powders are intensively used in modern electrical or optical devices where the large interfaces between the grains of the composite play a fundamental role. The interfaces are often the geometrical zones of interest and their percolation through a sample are primordial for the physical properties of a system. These heterogeneous media can be dispersed as a thin layer upon a substrate (superconducting layer, applications to furtivity, active skins as antenna) or they can occupy a three-dimensional (3D) volume. As related physical effects we could quote, for instance, the increase of conductivity of granular ionic conductors in which an insulating powder is dispersed between the grains [1], the behavior of wet brushite composites [2], and enhanced Raman scattering [3].

Percolation models are well adapted: the disordered systems, where an electromagnetic wave propagates are often modeled by random networks where each bond represents a grain or a grain boundary.

[a] e-mail: raymond@lrc.univ-mrs.fr

Here we only consider simple square (2D) or cubic (3D) lattices, but the method is straightforwardly applicable to any simply connected network, regardless of its dimensionality.

The notations of this paper are those of [4,5] and we recall them shortly. The bond occupation is obtained according to the following binary law: conductance σ_0 and concentration p for one kind of bond, σ_1 and $1-p$ respectively for the other kind. The dimensionless complex ratio $h = \sigma_1/\sigma_0$ of the two conductances is *de facto* the essential parameter along with the concentration p. We will use the equivalent complex variable

$$\lambda = \frac{1}{1-h} = \frac{\sigma_0}{\sigma_0 - \sigma_1} \cdot \tag{1}$$

In the static (DC) case, the limit $h = 0$ ($\lambda = 1$) corresponds to the two possibilities: the two species are respectively conductor and insulator ($\sigma_1 = 0$), or conductor and super conductor ($\sigma_0 = \infty$). We are confronted with a classical percolation problem.

In the 2D case, the square lattice is self-dual, and quantities such as the percolation threshold can be easily deduced from this property. But the system is somewhat

Table 1. The resonance position and the corresponding residues are presented for some configurations (animals) consisting of one or two bonds: only one animal is put in different positions in a cubic lattice $8 \times 8 \times 8$. With the boundary conditions, only the current direction is relevant. The name i_n points out a bond alone between the rows n and $n+1$ ($n=0$ is the top electrode at potential V_0). I_n represents two bonds in the same direction, between the rows n and $n+2$.

animal	pole position	residue 10^{-2} unit
i_0, i_7	0.789308423	4.17081055
i_1, i_6	0.674277363	7.54795650
i_2, i_5	0.668037619	7.76440136
i_3, i_4	0.667363895	7.78801367
I_0, I_6	0.570490690	0.77324464
	0.893095096	3.61773483
I_1, I_5	0.544761964	0.00397830
	0.797553018	7.93113971
I_2, I_4	0.543267933	0.00004814
	0.792133581	8.20040186
I_3	0.543157473	0
	0.791570318	8.22848890

Table 2. See table 1: similar results for an animal Γ_n made of two perpendicular bonds with the vertex on the row $n+1$.

animal	pole position	residue 10^{-2} unit
Γ_0	0.566366254	4.05530700
	0.903637749	1.10140027
Γ_1	0.534390544	6.66404562
	0.808411116	1.89039118
Γ_2	0.531898275	6.86342706
	0.803701317	1.91149019
Γ_3	0.531617073	6.88538519
	0.803195822	1.91366884
Γ_4	0.531730016	6.88512684
	0.803195852	1.91287160
Γ_5	0.532860589	6.86124029
	0.803701327	1.90472208
Γ_6	0.546552694	6.64049976
	0.808420249	1.80603241

pathological: the threshold p_c coincides with a symmetry point $p=0.5$ where the two species of the binary compound are equally represented.

In 3D, the self-duality property is lost, and even the notion of duality is not easy to define because the dual of a bond lattice is not a bond lattice. Nevertheless, independently of self-duality, a symmetry around $p=1/2$ value always holds for binary systems, regardless of the geometry of the network. Namely, swapping the two impedances and changing p in $1-p$ always leaves a binary system unchanged.

For a cubic lattice the percolation threshold for σ_0 links is given by $p_\mathrm{c}=0.2488126$ [6]. The percolation thresholds are obtained for the two species (σ_0 and σ_1) at respectively p_c and $1-p_\mathrm{c}$. At the symmetry point ($p=1/2$), σ_0 and σ_1 sub-lattices both percolate and the system is far from transition points.

In the vicinity of the critical points, *i.e.* for $|h| \ll 1$ and $|p-p_\mathrm{c}| \ll 1$, the sample conductivity obeys a scaling law. It is well-known that the conductivity is given by the second order moment of the intensity $\sum_{(x,y)} I_{xy}^2$ where I_{xy} is the current flowing from the node x to the node y. We will verify that, as in the 2-D case [7], the different moments of the intensity obey a multi-fractal scaling law. The impedance of the random networks can also be evaluated for frequency dependent systems with complex conductivities affected to the bonds of the regular lattice.

We have to solve the Kirchhoff equation at the different nodes x of the network:

$$\sum_{y(x)} \sigma_{x,y}(V_x - V_y) = \sum_{y(x)} I_{x,y} = I_x \qquad (2)$$

where V_x correspond to the potential on the node x and $I_{x,y}$ is the current from x to y along the link of conductance $\sigma_{x,y}$.

If a current I flows through the sample between two planar electrodes, one at a potential V_0 and the other one grounded, the conductance of the network reads $Y = I/V_0$. For a finite system, the conductance of the network takes the form $Y = N(\lambda)/D(\lambda)$ where N and D are polynomials whose degrees are roughly equal to the number of bonds of the network. The poles and the zeros of the conductance alternate on the negative real axis of the complex parameter h, or equivalently in the interval $[0,1]$ of the real axis in the λ plane [8]. The poles for the conductance, named resonances, are obtained for frequencies corresponding to $\lambda = \lambda_a$ values. They can be physically interpreted as a vanishing V_0 for non-vanishing I.

For a given network, a very complicated spectrum of resonances, characteristic of the geometry of the sample, is obtained by solving numerically a generalized eigenvalue problem equivalent to the Kirchhoff equations. This approach, first proposed by Straley [9], allows the calculation of the conductivities, corresponding to different values of h. The determination of the poles of the conductance and the corresponding residue is required. One must average a large number of samples in order to obtain information intrinsic to the composition p. One can also consider a small given cluster ("animal"), of say some connected conducting bonds, in a sea of insulating bonds [5]. It is easy to obtain the resonant set for this animal (see Tab. 1). Its contribution can then be identified in the overall spectrum of a macroscopic binary heterogeneous system. In applications, a pattern could be chosen in order to obtain a selective absorption or reflectivity for a given frequency bandwidth with applications for instance in the construction of planar antennas.

The paper is organized as follows. In Section 2, we present our notations and the numerical algorithm. In

Section 3, the results are presented and discussed. We conclude the paper by proposing some applications of 3D binary random networks.

2 Model and methodology

We model the electrical properties of a compressed powder by considering that the grains are on the vertices of a lattice, in contact along the links. For example, we put a capacity to represent a bad conducting contact between two grains, and a resistance (possibly inductive) for a good contact. The sample is thus seen as a random impedance network.

We restrict ourselves to a binary network, using only two values for the impedance of a link. With more possible values the problem is undoubtly interesting but unfit for the spectral method we use here.

As the set of sites, we consider a finite piece L of the cubic lattice, namely

$$L = \{1 \dots N_x\} \times \{1 \dots N_y\} \times \{1 \dots (N_z - 1)\}\,.$$

We take the planes $z = 0$, and $z = N_z$ as electrodes (any pair of sites in each of these two planes are connected by an infinitely conducting link). Finally, between two nearest neighbors, we put a link of impedance σ_0 (type P link) with probability p, and a link of impedance σ_1 (type Q link) with probability $q = 1 - p$. We consider periodic boundary conditions in the (x, y) plane, in order to try to reduce the finite-size effects in the numerical computation.

We are, of course, not interested in a particular realization of the network. We will always average the studied quantities over a sufficient number of realizations of the disorder. By this averaging procedure, we expect to obtain more information on a real (almost infinite) system. It is known, for such a model, that p (the density of type P links) and $h = \frac{\sigma_1}{\sigma_0}$ are the relevant macroscopic parameters for the determination of the averaged quantities we are interested in.

For obvious symmetry considerations, the exchange of p and q corresponds to replacing h by $\frac{1}{h}$. Instead of h itself, it is more practical to use $\lambda = \frac{1}{1-h}$. Then the above transformation corresponds to a change of λ in $1-\lambda$. This symmetry allows us to restrict the range of investigation of such models to $p \leq \frac{1}{2}$. Moreover, one can immediately conclude that any averaged quantity computed for $p = \frac{1}{2}$ will be symmetrical around the value $\lambda = \frac{1}{2}$. For instance, one can compute the average conductance of the network

$$Y(p, \sigma_0, \sigma_1) = \sigma_0 \tilde{Y}(p, \lambda) = \sigma_1 \tilde{Y}(1 - p, 1 - \lambda). \qquad (3)$$

For each given realization, the conductance of the network, $Y_0(\lambda)$, is a rational fraction with isolated singularities in the interval $[0, 1]$. It has only simple poles with non-negative residues, and can be thus written in the Bergman-Milton integral representation [8]:

$$Y_0(\lambda) = \sum_{a \in \mathcal{A}} \frac{\gamma_a}{\lambda - \lambda_a}\,\cdot \qquad (4)$$

It is conjectured that for an infinite-size network, the whole interval becomes a singular line for the conductance (we make the same conjecture for the conductance averaged on an infinite number of realizations). If one assumes this result, the conductance is completely determined by the density of singularities in the complex plane. See [10] and references therein for more details on this spectral representation. Namely, the averaged conductance of a finite-size network is written as

$$\frac{\tilde{Y}(p, \lambda)}{\tilde{Y}(p, \infty)} = \int_0^1 \mathrm{d}x \frac{n(p, x)}{\lambda - x} + 1, \qquad (5)$$

where $\sigma_0 \tilde{Y}(p, \infty)$ is the conductance of the uniform network ($\sigma_0 = \sigma_1$),

$$\tilde{Y}(p, \infty) = \frac{N_x N_y}{N_z}\,\cdot \qquad (6)$$

To get a numerical approximation for the *spectral density* $n(p, x)$, we construct an histogram in the following way. We cut the $[0, 1]$ interval in small intervals I_k, and we compute the integrals of $n(p, x)$ on each I_k. For a given realization, a pole λ_a of $\tilde{Y}$ which falls in I_k contributes to the integral with a weight given by the corresponding residue γ_a. By this procedure, one gets a staircase function which approximates the spectral density.

The numerical problem is thus reduced to the computation of the positions and amplitude of the resonances. We show in Appendix A how they are related to the generalized eigenvalues and eigenvectors of a Laplacian-like matrix. The computation can be done using a classical numerical method. One can then obtain the resistance of the network for any ratio h of local conductances, or equivalently, for any frequency, if a frequency-dependent ratio is under study. It is thus easy to draw a Cole-Cole diagram for the network which can be fitted with experimental measurements on a real sample.

The numerical results have been compared, for positive (real) values of h, with those obtained by a direct resolution of the Kirchhoff equations. The agreement was excellent. The method also allows a self-checking. It can be verified, for each configuration, that the incoming current is equal to the outgoing current. The difference gives an order of magnitude for the numerical precision.

3 Results and discussion

We present some results obtained, as a function of λ, for a given value of the composition. The calculations are done at the threshold $p = p_c$. The four graphs of Figure 1 are: the pole density, the spectral density as defined in Section 2, the sum

$$\Sigma_a = \lambda_a n(p, \lambda_a)$$

representing an average position of resonances, and the weight of each resonance. The graphs contain several curves, corresponding to different sizes of the samples. Results are averaged on a number of realizations such that the total number of considered random links is about 5×10^6.

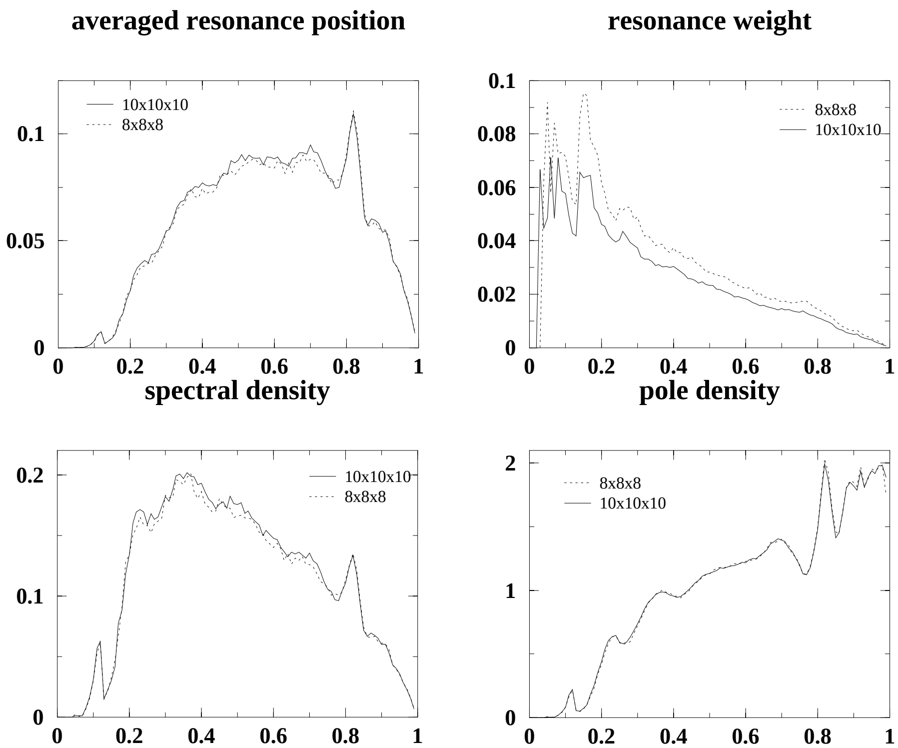

Fig. 1. Example of graphs for $p = p_c$ and linear sizes of 8 and 10.

We observe in Figure 1 a very poor convergence of the resonance weight when the linear size of the network varies from eight to ten, especially for the small values of λ. The statistics is very inaccurate because there are too few poles in this region. But the disagreement is not really bothering because the quantity of interest for the calculation of the conductivity is the spectral density, *i.e.* the product of the resonance weight with the pole density (which is a very small quantity in this region).

Figure 1 also shows that the spectral density has reached a good convergence for a very small 3D sample size. Here we obtain nearly the same results for the two linear sizes: $N_x = N_y = N_z = 8$ and 10.

For very "dilute" samples ($p \ll 1$), one can easily identify the contributions from elementary animals such as isolated links or pairs of links. The resonances and their weights (residues) corresponding to several animals are presented in Table 1. If a given animal is predominant in a given network, it is easy to predict the conductivity ratio h, and then the frequency, which leads to the optimal conductivity. Some interesting practical properties could originate from this remark. Most peaks in the pole density are centered on characteristic values for well-known animals. The number of patterns generated in a random sample increases quickly with the density and it is thus more and more difficult to assign the observed structure to given animals.

The resonance positions given in Table 1 can be compared with the values obtained for the same animal in a infinite network by the method described in [4] for a 2D case. Following this method, one obtains the positions of resonances for a given animal as the eigenvalues of a matrix obtained from the values of the Green function of the laplacian operator on the infinite lattice. This method can be easily extended to the 3D systems, with the restriction that one cannot compute analytically the values of the entries of this matrix except for some cases such as the isolated link.

i) *An isolated link*: One has to compute the eigenvalues of

$$M = \frac{1}{6}\begin{pmatrix} 1 & -1 \\ -1 & 1 \end{pmatrix},$$

the obtained value ($\lambda = \frac{1}{3}$) correspond to a type Q link in an infinite lattice of type P links. The values given in Table 1, correspond to animals of type P links. One has to compute $1 - \lambda = \frac{2}{3}$ to make a comparison. Agreement is thus obtained with the value for i_3 in Table 1 up to the third digit.

ii) *A pair of adjacent links*: For a pair of adjacent links, the matrix to be considered is

$$M = \frac{1}{6}\begin{pmatrix} 1 & -(2+6g) & 6g+1 \\ -1 & 2 & -1 \\ 6g+1 & -(2+6g) & 1 \end{pmatrix},$$

the value of g is computed numerically. It depends on the relative orientation of the two links. One obtains $\lambda_1 = -g$ and $\lambda_2 = g + \frac{2}{3}$ as eigenvalues of M leading to resonances at $1+g$ and $\frac{1}{3} - g$. For two links with the same orientation, $g \approx -0.2098$, the two resonances are respectively 0.7902 and 0.5431 in accordance with the computed values for I_3 up to 2 digits. For two orthogonal links, $g \approx \frac{-1+0.2098}{4} \approx -0.1976$. The resonances are around 0.5301 and 0.8025 again in accordance with the values for Γ_3 in Table 1 up to 2 digits.

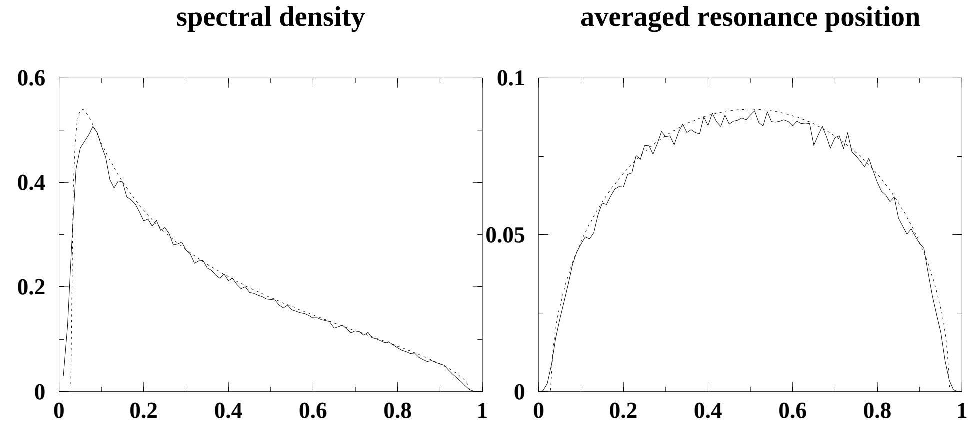

Fig. 2. Pole density and average resonance position at $p = 0.5$, for a linear size of 8 (solid line), and EMA curve (dotted line).

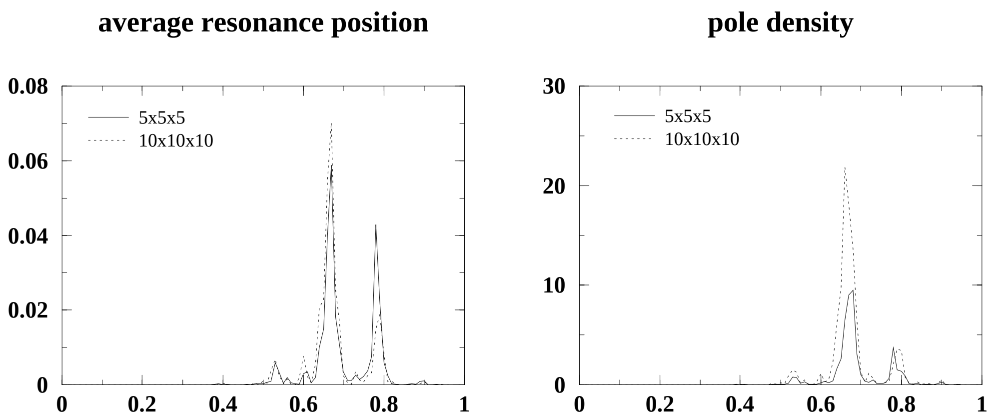

Fig. 3. Pole density and average resonance position for linear sizes of 5 and 10 at $p = 0.01$ (very dilute sample).

The averaged resonance position presents a noticeable property: in the effective medium approximation (EMA) [11] its representation *versus* λ is a semi-circle. The EMA model is a coarse but very useful approximation. It is still widely used [7,12]. It gives a good qualitative idea of the behavior exhibited by a system and works better when the fluctuations can be neglected. The comparison of the averaged resonance histogram gives a good idea of the ability for the EMA to work as a good approximation. Figure 2 shows that this result is reached in the 3D case for $p = 0.5$ and corresponds to a smooth contribution of the eigenvalues: all the animals are represented with comparable weight. The averaged resonance is invariant with the simultaneous interchange $p \leftrightarrow q = 1-p$ and $\lambda \leftrightarrow 1-\lambda$.

We do not have self-duality in the 3D case as in the 2D case. For this reason the various functions represented in Figure 1 are not symmetrical with respect to $\lambda = 0.5$ as they were for a 2D model. It is surprising that the 2D model gives the same good agreement between the EMA and the simulation results for $p = 0.5$, because this value corresponds also, by accident, to the bond percolation threshold where the fluctuations diverge. So the validity of the EMA model seems in that case related to the symmetry of the network instead of the density value at the percolation threshold. In Figure 3, the pole density and average resonance position are represented *versus* λ, illustrating a typical finite-size effect coming from the contribution of a single link attached to an electrode. The corresponding peak is observed for $\lambda \simeq 0.8$ in Figure 3. The pole density and average resonance position scale as the inverse of the linear size of the sample, which corresponds to the ratio surface over volume for a cubic sample. This is the expected result of the linear decreasing contribution of the surface effects when the sample size increases. Conversely, on the same curves, the peak in the vicinity of $\lambda \simeq 0.65$ corresponds to isolated bonds in the bulk which is independent of the size of the sample.

The spectral method also provides a direct determination of the distribution of the local electric field $E_{x,y} = V_x - V_y$. More precisely, we evaluate for cubic samples of size $N \times N \times N$ the mean values of the k-moments $\Sigma_{(x,y)}|E_{x,y}|^k$. The results are normalized with a multiplicative constant C such that $C = \Sigma_{(x,y)}E^2_{x,y}$ and we look at the quantity $S_k(N)$ defined as:

$$\frac{1}{C}\langle \Sigma_{(x,y)}|E_{x,y}|^k\rangle,$$

where k is an integer varying from one to six. We can extend the definition to $k = 0$ by summing over all bonds (x, y) such that $E_{x,y} \neq 0$.

For instance, in a simple static superconductor-conductor system ($\sigma_0 \mapsto \infty$ and σ_1 finite), the electric field

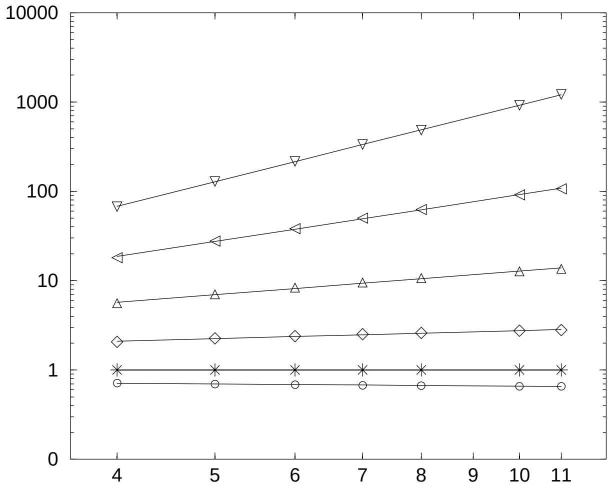

Fig. 4. Log-log plot of the moments $S_k(N)$ with $k = 1$ to 6, *versus* the sizes N of the samples. The slopes are: -0.0832 for $k = 1$ ($\circ$), 0 (definition) for $k = 2$ ($*$), 0.2981 for $k = 3$ ($\diamond$), 0.8724 for $k = 4$ ($\triangle$), 1.7400 for $k = 5$ ($\triangleleft$), 2.8463 for $k = 6$ ($\bigtriangledown$).

does not vanishes only on the conducting bonds, where the electric field is proportional to the current. The moment for $k = 0$, in this limit approach the mean density of conducting bonds in the sample. S_2 converges to the conductivity of the conducting path and, for increasing values of k, the high currents are privileged. S_6 gives a good idea of the average density of *red bonds* in the conducting path because by definition the maximal (finite) current flows through the red bonds.

For the general AC problem, the variation of the k moments *versus* the sample size is close to a power law with the exponents x_k [7]. In the caption of Figure 4, we give the x_k's. They do not obey a linear relation $x_k \neq x_0 + \alpha k$. This property indicates that the distribution of the local electric fields has a multi-fractal nature.

One can associate to the x_k a quantity d_k related in some sense to fractal dimensions of the set of links with a significant potential value. We define $d_k = 3 - x_k \frac{2}{k-2}$ for $k \neq 2$. We can expect a linear behavior $d_k \equiv 3 - \beta k$ where β is roughly 0.25 for the cubic lattice [13]. One can observe, on the graph of Figure 5, this linear behavior of d_k as a function of k, with $\beta = 0.253 \pm 5 \times 10^{-3}$, compatible with the expected value. There exists nevertheless a noticeable discrepancy between the $k = 0$ value ($d_0 = 3$) and the observed one $\tilde{d_0} = 3.12 \pm 2 \times 10^{-3}$.

4 Conclusion

As noted in [7,4], the spectral method is particularly interesting for repetitive calculations with numerous conductance ratios: when the spectral density corresponding to a given sample is memorized, it can be used to calculate the conductance for every value of h (or λ). Therefore, for the investigation of frequency-dependent quantities, this algorithm is more suitable than the classical ones, as sparse matrix method [14], transfer matrix method [15] or the star-triangle transformation [16].

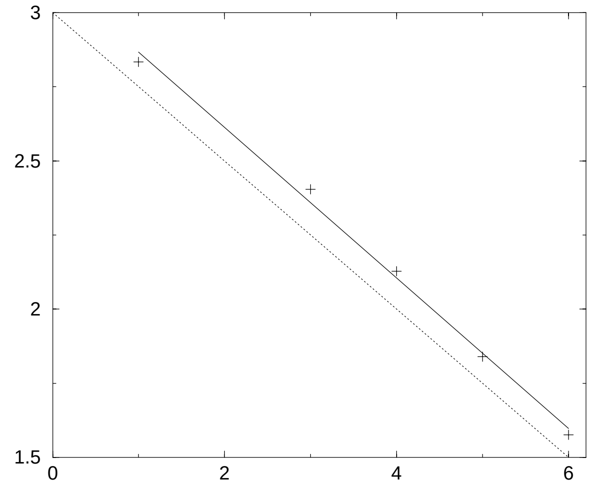

Fig. 5. Dimensions d_k associated to the scaling exponents x_k *versus* k (+), linear fitting with slope $0.253 \pm 5 \times 10^{-3}$ and intercept $3.12 \pm 2 \times 10^{-3}$ (solid line) and expected values (dotted line).

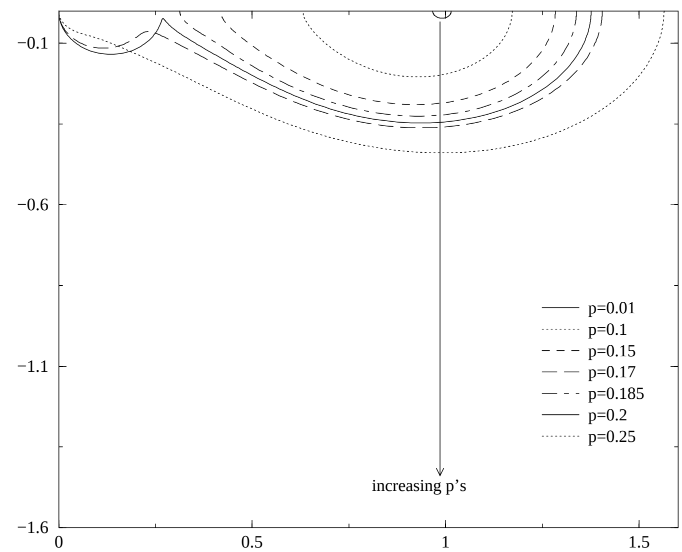

Fig. 6. Frequency variation of the impedance (real part *versus* imaginary part) of a $8 \times 8 \times 8$ cubic array of capacitors bonds, doped with several concentrations p of resistors bonds.

As an illustration, and in order to allow a simpler comparison with experiments, we give here the Cole-Cole diagram obtained for a cubic lattice of resistors ($\sigma_0 = R^{-1}$), doped with a density p of capacitors ($\sigma_1 = jC\omega$). The results are presented for $R = 1$, $C = 1$ and are averaged on a collection of $8 \times 8 \times 8$ samples, for densities varying from $p = 0.01$ to $p = 0.5$.

Figure 6 shows that for a very small amount of capacitors ($p = 0.01$), the Cole-Cole diagram is a perfect semi-circle centered on the value R corresponding to the DC resistivity of the sample. When p is increased, but not sufficiently to allow any percolating paths of capacitors, the semi-circle is slightly distorted at high frequency (*i.e.* in the vicinity of the real axis close to the origin). We also see that for higher p's, another semi-circle ending on the origin appears. This is characteristic of a percolating capacitors path, and should not be visible for p's less than the percolation threshold. This is thus the signature of a finite size effect, roughly speaking, for a p between 0.17 and 0.25, where the Cole-Cole diagram is the superposition of two semi-circles corresponding to percolating and non percolating samples. The ratio of the radius of the two semi-circles is related to the percolation probability for a finite size sample.

In this paper, the work presented in [7] is straightforwardly extended to the 3D case in order to give a more relevant description of binary composite materials. Indeed, in practical realizations, the thickness of a painting layer can be much larger than the wavelength of an incident electromagnetic wave.

Progress in furtivity, active skins, giant Raman scattering could be the spin-offs of a good understanding of the behavior of composite materials in an electromagnetic field. For instance, the knowledge of the resonances associated to a given pattern allows to construct a skin which absorbs an incident electromagnetic wave of well-defined wavelengths. By combining several animals, one could obtain an arbitrary set of resonances, leading to an arbitrary frequency response of the painted object.

It is a real pleasure to thank J.P. Clerc and J.M. Luck for very enlightening discussions, P. Knauth and A.M. Tremblay for their very careful reading of the manuscript.

Appendix A: Total conductance computation

To compute the potential on the sample, one has to solve the Kirchhoff equations,

$$\sum_y \sigma_{xy}\,(V_x - V_y) + \sigma_x^u(V_x - V^u) + \sigma_x^d(V_x - V^d) = 0 \ \ \forall x. \tag{A.1}$$

Where σ_{xy} denotes the conductance between two sites x and y, and σ_x^{u}, the conductance from the site x to the upper electrode at potential V^{u} (d refers to the bottom electrode). We always assume that the bottom electrode's potential is fixed by $V^{\mathrm{d}} = 0$. We define $P(x)$ as the set of sites linked to x by a σ_0 conductance and $Q(x)$ those linked by a σ_1. We set $\chi_x^{\mathrm{u}} = 1$ if x is linked to the upper electrode, and 0 elsewhere. Similarly, we define $B_x^{\mathrm{u}} = 1$ if there is a link of conductance σ_1 from x to the upper electrode. Note that $\sigma_x^{\mathrm{u}} = \sigma_0(\chi_x^{\mathrm{u}} - \frac{1}{\lambda}B_x^{\mathrm{u}})$. Equation (A.1) becomes

$$\sigma_0 \sum_{y\in P(x)} (V_x - V_y) + \sigma_1 \sum_{y\in Q(x)} (V_x - V_y) + \sigma_x^{\mathrm{u}}(V_x - V^{\mathrm{u}}) + \sigma_x^{\mathrm{d}}(V_x - V^{\mathrm{d}}) = 0. \tag{A.2}$$

This suggest a Laplacian operator formulation involving only the λ parameter. In this setting, equation (A.1) is cast into

$$(-\Delta_Q V)_x - \lambda(-\Delta V)_x = (B_x^{\mathrm{u}} - \lambda\chi_x^{\mathrm{u}})\,V^{\mathrm{u}}\,,\ \forall x \in L\,. \tag{A.3}$$

Where the Laplacian Δ, is defined by $\Delta_{xy} = 1$ if there is a link between x and y, $-\Delta_{xx}$ is the number of links starting from the site x, including links from x to an electrode (note the $-$ sign). The matrix Δ_Q is defined in the same way, but one considers only the type Q links (σ_1 conductance).

The problem can now be solved by considering the generalized eigenvalue equation for the operators $(-\Delta_Q)$ and $(-\Delta)$. Namely, one has to find all possible generalized eigenvalues λ_a and an associated orthogonal basis of generalized eigenvectors $V(\lambda_a)$ such that

$$\begin{aligned}(-\Delta_Q)V(\lambda_a) &= \lambda_a(-\Delta)V(\lambda_a),\ a \in \mathcal{A}\,,\\ \langle V(\lambda_a)^\dagger|(-\Delta)V(\lambda_b)\rangle &= \delta_a^b,\ a, b \in \mathcal{A}.\end{aligned} \tag{A.4}$$

Where, $\dagger$ denotes the hermitic conjugation, $\langle V^\dagger|W\rangle = \sum_{x\in L} V_x^\dagger W_x$ is the usual scalar product, δ is the Kroenecker symbol and $\mathcal{A}$ is a set of indices (*e.g.* integers between 1 and n_r, the number of eigenvalues counted with multiplicities). Note that this generalized eigenvalue problem is always solvable because $(-\Delta)$ is a (positive) definite operator thus invertible. Moreover, $(-\Delta_Q)$ and $(-\Delta)$ are self-adjoint operators, thus, all the λ_a's and all components of the $V(\lambda_a)$'s are real numbers. One can even show that all the λ_a's fall in the $[0, 1]$ interval, using the fact that $(-\Delta_Q)$ and $(-\Delta_P) = (-\Delta) - (-\Delta_Q)$ are also positive operators.

The Kirchhoff equations can now be solved by expanding the solution $V(\lambda)$ for a given λ on the orthonormal basis of eigenvectors of $(-\Delta_Q)$. Indeed, one sets

$$V(\lambda) = \sum_{b\in\mathcal{A}} c_b(\lambda)V(\lambda_b), \tag{A.5}$$

then substitutes this expression in equation (A.3)

$$V^{\mathrm{u}}(B^{\mathrm{u}} - \lambda\chi^{\mathrm{u}}) = \sum_{b\in\mathcal{A}} c_b(\lambda)\left((-\Delta_Q)V(\lambda_b) - \lambda(-\Delta)V(\lambda_b)\right), \tag{A.6}$$

then by (A.4) one can obtain the coefficient $c_a(\lambda)$ for a given a by taking the scalar product with $V(\lambda_a)^\dagger$. Indeed

$$\begin{aligned}V^{\mathrm{u}}\langle V(\lambda_a)^\dagger|B^{\mathrm{u}} - \lambda\chi^{\mathrm{u}}\rangle &= V^{\mathrm{u}}\left[(\lambda_a - \lambda)\langle V(\lambda_a)^\dagger|\chi^{\mathrm{u}}\rangle + \langle V(\lambda_a)^\dagger|B^{\mathrm{u}} - \lambda_a\chi^{\mathrm{u}}\rangle\right]\\ &= (\lambda_a - \lambda)c_a(\lambda).\end{aligned} \tag{A.7}$$

We define $\mathcal{A}_0$ the set of indices a such that $\lambda_a = 0$. It will be proven in the next section that

$$\langle V(\lambda_a)^\dagger|B^{\mathrm{u}}\rangle = \langle V(\lambda_a)^\dagger|B^{\mathrm{d}}\rangle = 0,\ \forall a \in \mathcal{A}_0. \tag{A.8}$$

This property of eigenvectors in the kernel of Δ_Q allows one to exclude all the terms $\langle V(\lambda_a)^\dagger|B^{\mathrm{d}}\rangle$ for $a \in \mathcal{A}_0$ in the sum. Moreover, the exchange of σ_0 and σ_1 is equivalent to the exchange of the P set and the Q set. This implies that the system is invariant under the transformation

$\lambda \mapsto (1-\lambda)$ and $\Delta_Q \mapsto \Delta_P = (\Delta - \Delta_Q)$. Thus, if one defines $\mathcal{A}_1$ the set of indices a such that $\lambda_a = 1$, all terms $\langle V(\lambda_a)^\dagger | B^{\mathrm{d}} - \lambda_a \chi^{\mathrm{d}} \rangle$ vanish for a in $\mathcal{A}_1$. This suggest the use of the set $\tilde{\mathcal{A}}$ of all indices which are neither in $\mathcal{A}_1$ nor in $\mathcal{A}_0$.

Finally one gets for the potential on the lattice

$$V(\lambda) = V^{\mathrm{u}}(-\Delta)^{-1}\chi^{\mathrm{u}} + V^{\mathrm{u}} \sum_{a\in\tilde{\mathcal{A}}} \frac{\langle V(\lambda_a)^\dagger | B^{\mathrm{u}} - \lambda_a \chi^{\mathrm{u}}\rangle}{\lambda_a - \lambda} V(\lambda_a), \qquad (\mathrm{A.9})$$

using the identity, holding for any vector W,

$$\sum_{a\in\mathcal{A}} \langle V(\lambda_a)^\dagger | W \rangle V(\lambda_a) = (-\Delta)^{-1} W\,. \qquad (\mathrm{A.10})$$

Note that for the uniform lattice ($p = 1$), the potential is given by $V^{\mathrm{u}}(-\Delta)^{-1}\chi^{\mathrm{u}}$. Thus equation (A.9) gives the solution of the Kirchhoff equations as a deviation from the potential on the pure P-type lattice.

One can now compute the intensity flowing through the sample (and thus its conductance) by summing all the contributions on the links between the lower electrode and the lattice.

$$I = YV^{\mathrm{u}} = \sum_{x\in L} \sigma_x^{\mathrm{d}}\,(V_x)\,. \qquad (\mathrm{A.11})$$

Here one has to substitute σ^{d} by its expression in term of λ,

$$\sigma_x^{\mathrm{d}} = \sigma_0 \chi_x^{\mathrm{d}} - (\sigma_0 - \sigma_1) B_x^{\mathrm{d}} = \frac{\sigma_0}{\lambda}\left(\lambda \chi_x^{\mathrm{d}} - B_x^{\mathrm{d}}\right). \qquad (\mathrm{A.12})$$

This leads to the following form for the conductance

$$\frac{Y(\lambda)}{\sigma_0} = \left\langle \left(\chi^{\mathrm{d}} - \frac{B^{\mathrm{d}}}{\lambda}\right)^\dagger \middle| \frac{V(\lambda)}{V^{\mathrm{u}}} \right\rangle. \qquad (\mathrm{A.13})$$

Then one defines the reduced conductance of the sample $\tilde{Y} = \frac{N_z Y}{N_x N_y \sigma_0}$ which reads

$$\tilde{Y}(\lambda) = \frac{N_z}{N_x N_y} \left\langle \left(\chi^{\mathrm{d}} - \frac{B^{\mathrm{d}}}{\lambda}\right)^\dagger \middle| (-\Delta)^{-1}\chi^{\mathrm{u}} + \sum_{a\in\tilde{\mathcal{A}}} \frac{\langle V(\lambda_a)^\dagger | B^{\mathrm{u}} - \lambda_a \chi^{\mathrm{u}}\rangle}{\lambda_a - \lambda} V(\lambda_a) \right\rangle. \qquad (\mathrm{A.14})$$

This last expression can be simplified by use of the properties of $(-\Delta)^{-1}\chi^{\mathrm{u}}$. Recall that it is constant and equal to $\frac{z}{Nz}$ on the plane at altitude z (parallel to the electrode). One has

$$\left\langle \left(\chi^{\mathrm{d}}\right)^\dagger \middle| (-\Delta)^{-1}\chi^{\mathrm{u}} \right\rangle = \frac{N_x N_y}{N_z}\,. \qquad (\mathrm{A.15})$$

After further simplification, the conductance reduces to

$$\tilde{Y}(\lambda) = 1 - \frac{N_z}{N_x N_y}\left[\frac{1}{\lambda} \sum_{a\in\mathcal{A}-\mathcal{A}_0} \frac{\langle (B^{\mathrm{d}})^\dagger | V(\lambda_a)\rangle \langle V(\lambda_a)^\dagger | B^{\mathrm{u}}\rangle}{\lambda_a} - \sum_{a\in\tilde{\mathcal{A}}} \frac{\langle \left(B^{\mathrm{d}} - \lambda_a\chi^{\mathrm{d}}\right)^\dagger | V(\lambda_a)\rangle \langle V(\lambda_a)^\dagger | B^{\mathrm{u}} - \lambda_a\chi^{\mathrm{u}}\rangle}{\lambda_a(\lambda_a - \lambda)}\right]. \qquad (\mathrm{A.16})$$

Consequently, because

$$\begin{aligned} 0 &= \sum_{x\in L} ((-\Delta_Q) - \lambda_a(-\Delta)) V(\lambda_a) \\ &= \langle \left(B^{\mathrm{d}} - \lambda_a\chi^{\mathrm{d}}\right)^\dagger | V(\lambda_a)\rangle + \langle \left(B^{\mathrm{u}} - \lambda_a\chi^{\mathrm{u}}\right)^\dagger | V(\lambda_a)\rangle. \end{aligned} \qquad (\mathrm{A.17})$$

One gets the equivalent expression

$$\tilde{Y}(\lambda) = 1 - \frac{N_z}{N_x N_y}\frac{1}{\lambda}\left[N_Q^{\mathrm{u}} - \sum_{a\in\mathcal{A}-\mathcal{A}_0} \frac{\left|\langle (B^{\mathrm{u}})^\dagger | V(\lambda_a)\rangle\right|^2}{\lambda_a}\right] + \frac{N_z}{N_x N_y} \sum_{a\in\tilde{\mathcal{A}}} \frac{\left|\langle \left(B^{\mathrm{u}} - \lambda_a\chi^{\mathrm{u}}\right)^\dagger | V(\lambda_a)\rangle\right|^2}{\lambda_a(\lambda_a-\lambda)}\cdot \qquad (\mathrm{A.18})$$

This last expression is nothing but the Laurent series expansion of $\tilde{Y}(\lambda)$. It shows that $\tilde{Y}(\lambda)$ is a rational function with only simple poles. It is also an alternative way to prove that it is a Stielges function, namely that imaginary parts of $\tilde{Y}(\lambda)$ and λ have the same sign [8,7].

Appendix B: Pole at the origin

We will prove in this appendix that the vanishing eigenvalue has no influence on the residue value of the pole at the origin. This means physically that it has no influence on the unpowered sample's behavior, and proves the assertion in [7] that the resonances at $\lambda = 0$ and $\lambda = 1$ are unphysical.

Let V be an eigenvector of $-\Delta_Q$ with vanishing eigenvalue. Let's rewrite the eigenvalue equation $(-\Delta_Q)V = 0$ as

$$\sum_{y\in L} A_{xy}^{(0)} V_y = 0,\ \forall x \in L. \qquad (\mathrm{B.1})$$

We set $B_x^{(0)} = B_x^{\mathrm{u}} + B_x^{\mathrm{d}}$ the characteristic function of the type "Q" electrode's neighborhood. Note that $A^{(0)}$ is a symmetric matrix. Moreover, $A_{xx}^{(0)} \geq 0$, $A_{xy}^{(0)} \leq 0$ for $x \neq y$ and $\sum_y A_{xy} = B_x \geq 0$ by positivity of $(-\Delta_Q)$.

We will prove that for all x of the lattice, $B_x^{(0)} V_x = 0$ for any V such that $\Delta_Q V = 0$ (*i.e.* such an eigenvector as a vanishing value on any site linked to an electrode by a type Q impedance). Note that it has to be proven only for sites x such that $B_x^{(0)} \neq 0$, *i.e.* the sites linked to an electrode by a Q-type impedance.

The proof uses a renormalization procedure (also called decimation). One can choose a x_1 in the lattice such that $A^{(0)}_{x_1 x_1} \neq 0$. Then by equation (B.1), one can compute V_{x_1} as a function of V_x's for all other sites x. Namely

$$V_{x_1} = \frac{1}{A^{(0)}_{x_1 x_1}} \sum_{x \notin \{x_1\}} A^{(0)}_{x_1 x} V_x . \tag{B.2}$$

One can then substitute the value of V_{x_1} in equation (B.1) and thus eliminate the site x_1 in the computation. This leads to a renormalized equation

$$\sum_{y \notin \{x_1\}} A^{(1)}_{xy} V_y = 0,\ \forall x \notin \{x_1\}, \tag{B.3}$$

where

$$\begin{cases} A^{(1)}_{xy} = A^{(0)}_{xy} - \dfrac{A^{(0)}_{x x_1} A^{(0)}_{x_1 y}}{A^{(0)}_{x_1 x_1}}, \\ B^{(1)}_{x} = B^{(0)}_{x} - \dfrac{A^{(0)}_{x x_1} B^{(0)}_{x_1}}{A^{(0)}_{x_1 x_1}}. \end{cases} \tag{B.4}$$

This first step can obviously be iterated. Decimation of the sites $x_1 \ldots x_{k+1}$ leads to the following renormalized operator

$$\begin{cases} A^{(k+1)}_{xy} = A^{(k)}_{xy} - \dfrac{A^{(k)}_{x x_{k+1}} A^{(k)}_{x_{k+1} y}}{A^{(k)}_{x_{k+1} x_{k+1}}}, \\ B^{(k+1)}_{x} = B^{(k)}_{x} - \dfrac{A^{(k)}_{x x_{k+1}} B^{(k)}_{x_{k+1}}}{A^{(k)}_{x_{k+1} x_{k+1}}}, \end{cases} \tag{B.5}$$

and to the renormalized eigenvalue equation

$$\sum_{y \notin \{x_1, \ldots x_{k+1}\}} A^{(k+1)}_{xy} V_y = 0,\ \forall x \notin \{x_1 \ldots x_{k+1}\}. \tag{B.6}$$

We now describe the behavior of the matrix elements under decimation. First, we consider the values near the electrodes. One can easily show that

$$B^{(k)}_x = \sum_{y \notin \{x_1 \ldots x_{k+1}\}} A^{(k)}_{xy} . \tag{B.7}$$

Another remarkable fact is that the renormalized laplacian operator $-\Delta_Q^{(k)}$ has the same positivity properties as the original one. Namely

$$\begin{aligned} &A^{(k)}_{xx} \geq 0\,, \\ &A^{(k)}_{xy} \leq 0,\ \forall x \neq y \\ &B^{(k)}_x \geq 0. \end{aligned} \tag{B.8}$$

The proof goes by recursion. The property is true for $k = 0$. Assume it is true for a given k, then for x and y different from any x_j, $j = 1 \ldots k+1$,

$$\begin{aligned} A^{(k+1)}_{xy} &= A^{(k)}_{xy} - \frac{A^{(k)}_{x x_{k+1}} A^{(k)}_{x_{k+1} y}}{A^{(k)}_{x_{k+1} x_{k+1}}} \leq A^{(k)}_{xy} \leq 0\,, \\ B^{(k+1)}_{x} &= B^{(k)}_{x} - \frac{A^{(k)}_{x x_{k+1}} B^{(k)}_{x_{k+1}}}{A^{(k)}_{x_{k+1} x_{k+1}}} \geq B^{(k)}_x \geq 0\,, \\ A^{(k+1)}_{xx} &= - \sum_{\substack{y \notin \{x_1, \ldots, x_{k+1}\} \\ \text{and } y \neq x}} A^{(k+1)}_{xy} + B^{(k+1)}_x \\ &\geq B^{(k+1)}_x \geq 0. \end{aligned} \tag{B.9}$$

Equation (B.9) will be useful for it tells that for any non-renormalized site x, if $B^{(0)}_x \neq 0$ then $B^{(k)}_x \neq 0$ for any k.

We can now prove that $V_x = 0$ for any site x such that $B^{(0)}_x \neq 0$, and any V such that $-\Delta_Q V = 0$. Indeed, one simply decimates $x_1 \ldots x_K$, all sites of type Q except x. Note that for all X_k's $A(0)_{x_k x_k}$ does not vanish for it is greater or equal to the number of sites linked to x_k by a type Q impedance. The last (Kth) decimation step leads to

$$A^{(K)}_{xx} V_x = 0\,. \tag{B.10}$$

By equation (B.9), $A^{(K)}_{xx} \geq B^{(K)}_x \geq B^{(0)}_x > 0$, and thus $V_x = 0$.

References

1. J.M. Debierre, P. Knauth, G. Albinet, Appl. Phys. Lett. **71**, 1335 (1997).
2. L. Tortet, J.R. Gavarri, J. Musso, G. Nihoul, J.P. Clerc, A.N. Lagarkov, A.K. Sarytchev, Phys. Rev. B **58**, (1998).
3. F. Brouers, S. Blacher, A.N. Lagarkov, A.K. Sarytchev, P. Gadenne, V.M. Shalaev, Phys. Rev. B **55**, (1997).
4. J.P. Clerc, G. Giraud, J.M. Luck, Th. Robin, J. Phys. A **29**, 4781 (1996).
5. J.P. Clerc, G. Giraud, J.M. Laugier, J.M. Luck, Adv. Phys. **39**, 191 (1990).
6. C.D. Lorenz, R.M. Ziff, Phys. Rev. E **57**, 230 (1998).
7. Th. Jonckheere, J.M. Luck, J. Phys. A **31**, 3687 (1998).
8. D.J. Bergman, Phys. Rep. **43**, 377 (1978); Phys. Rev. Lett. **44**, 1285 (1980); Phys. Rev. B **23**, 3058 (1981); Ann. Phys. **138**, 78 (1981).
9. J.P. Straley, J. Phys. C **12**, 2143 (1979).
10. A.R. Day, M.F. Thorpe, J. Phys. Cond. Matter **8**, 4389 (1996).
11. D.A.G. Bruggeman, Ann. Phys. (Leipzig) [Folge 5] **24**, 636 (1935).
12. S. Kirpatrick, Rev. Mod. Phys. **45**, 574 (1973).
13. V.I. Fal'ko, K.B. Efetov, Europhys. Lett. **32**, 627 (1995).
14. R.R. Tremblay, G. Albinet, A.-M.S. Tremblay, Phys. Rev. B **43**, 11546 (1991); Phys. Rev. B **45**, 755 (1992).
15. J.M. Normand, H.J. Hermannand, M. Hajjar, J. Stat. Phys. **52**, 441 (1988).
16. C.J. Lobb, D.J. Frank, Phys. Rev. B **30**, 4090 (1984); D.J. Frank, C.J. Lobb, Phys. Rev. B **37**, 302 (1988).